Liquid-Metal Embrittlement of the Heat-Affected Zone by Copper Contamination

The mechanism responsible for copper-contamination hot cracking in the weld heat-affected zone is identified as liquid-metal embrittlement

BY W. F. SAVAGE, E. F. NIPPES, AND M. C. MUSHALA

ABSTRACT. This investigation was undertaken to determine the mechanism responsible for the Cu-induced hot-cracking which can not be explained by contemporary theory.

The Gleeble thermo-mechanical testing device was used to perform constant-load, stress-rupture tests and short-time hot-ductility tests in order to determine the effects of temperature, atmosphere, stress, grain size, strain rate, and amount of Cu on the Cu-contamination hot cracking. These tests established that the hot cracking resulted from liquid-metal embrittlement by Cu contaminating the surfaces of several Fe- and Co-base FCC alloys. Copper contamination totaling only 0.003 mil (0.076 μm) in thickness was sufficient to cause hot cracking.

The following sequence of events satisfactorily explains this recently discovered form of heat-affected-zone hot cracking.

1. Minute amounts of Cu are transferred from Cu or Cu-alloy tooling to the work surface near the weld.
2. The heat of the weld melts the Cu which then causes hot cracking by liquid-metal embrittlement.

Introduction

In a previous investigation,[1] the Fe- and Co-base alloys that have a FCC structure at the melting point of Cu (1982.3 F, 1083 C) were found to be susceptible, whereas Ni-base superalloys were insensitive to copper-contamination cracking (CCC). These preliminary tests suggested that the mechanism of cracking was a form of liquid-metal embrittlement.

If liquid-metal embrittlement is to occur between a specific solid-liquid metal couple, three criteria must be met:[2]

1. A low mutual solubility between the liquid and solid metals.
2. No intermetallic compound formations between the solid-liquid metal couple.
3. A barrier to plastic flow in the base metal, which is also in contact with the liquid metal.

When fracture does occur, the following characteristics have been noted:[2]

1. The yield stress and the strain-hardening rate remain unaffected.
2. If the material is not notch-sensitive, crack propagation proceeds as long as the liquid exists at the tip of the crack. On the other hand, if the material is notch-sensitive, the crack (if it reaches a critical size) can propagate without a continuous supply of liquid at the crack tip.
3. The liquid-metal-embrittled crack path is generally intergranular.
4. The fracture stress and ductility are extremely sensitive to temperature, strain rate, grain size, composition of the solid, composition of the liquid, and thermo-mechanical history.

The role of liquid metals in promoting embrittlement has been successfully developed[2,3] to explain the embrittlement of FCC metals which have always been considered ductile and incapable of cleavage failure.

The ratio, R, of the maximum cleavage stress (σ_{max}) divided by the maximum shear stress (τ_{max}) determines whether a crystal is ductile or brittle.[4] Although there is no sharp transition point between ductile and brittle behavior, with $R \leq 5$ the metal would exhibit brittle failure, and for metals with $R > 5$, the failure would be ductile with extensive plastic flow.

Liquid-metal embrittlement is believed to result from the interaction of the liquid-metal atoms with those atoms which define the crack tip. When a normally ductile FCC metal is stressed in tension in the presence of certain liquid metals, this metal may fail in a completely brittle fashion. This implies that a liquid-metal atom at the crack tip lowers R to less than 5. Stoloff[5] has demonstrated that a reduction in σ_{max} at the crack tip is caused by the chemisorption of the liquid-metal atoms at the crack tip. If a continuous supply of liquid is available, the liquid maintains such an "atomically sharp" crack tip that the

W. F. SAVAGE is Professor of Metallurgical Engineering and Director of Welding Research, and E. F. NIPPES is Professor of Metallurgical Engineering, Rensselaer Polytechnic Institute, Troy, New York; M. C. MUSHALA, former Graduate Assistant at RPI, is now a Captain in the U.S. Air Force, Randolph Air Force Base, San Antonio, Texas.

stress concentration is great enough to cause continuous crack propagation.

The most widely accepted liquid-metal transport mechanism is based upon capillarity.[6,7] Calculations indicate that this mechanism could transport liquid-metal atoms at rates approximating the observed crack velocities.

Perrone and Liebowitz[7] have examined the fracture behavior in liquid-metal embrittlement in terms of the capillary-transport mechanism. In the analysis, consideration must be made for the irregular intergranular path normally encountered with the cracking. The capillary-transport velocity, V, can be related to crack length, L, by the following expression (when the appropriate correction factor[8] for the intergranular path of the crack is applied):

$$V = \frac{Tr\cos\theta}{3\pi\mu L} \qquad (1)$$

where T is the surface tension of the liquid, r is the distance between the crack surfaces, θ is the contact angle, and μ is the coefficient of viscosity.

The chemisorption model for liquid-metal embrittlement has successfully explained the many experimental observations reported in the literature. For example, if the solid metal exhibited more than a limited solubility with the liquid metal, the liquid metal could preferentially dissolve the base metal and blunt the crack tip, thereby reducing its effectiveness as a stress raiser.

A dislocation mechanism is probably responsible for the crack initiation in liquid-metal embrittlement. Once nucleated, the crack propagates in accordance with the previously described chemisorption model. The current theories for dislocation interactions in liquid-metal embrittlement are based on the following observations:

1. The susceptibility to embrittlement increases as the stacking-fault energy of the FCC base metal decreases.
2. The wetted fracture stress in the FCC solid base metal generally increases with $d^{-1/2}$, where d is the average grain diameter (linear Petch dependence).
3. The transition temperature of the brittle-to-ductile transition of the wetted FCC metals generally increases with ln d.

The brittle-to-ductile transition has been explained by Preece,[9] who states that the chemisorption of the liquid-metal atom at the crack tip is a thermally-activated process. Because the rate of chemisorption decreases with increasing test temperature, the effectiveness of the liquid-metal atom in lowering σ_{max} at the crack tip would also decrease with increasing test temperature. Hence, the return of ductility results from an effective increase in the wetted cohesive bond strength, which would increase the ratio of σ/τ.

The severity of liquid-metal embrittlement has been shown to be decreased by the presence of an intervening oxide layer on the surface of the base metal.[6] This lack of liquid-metal embrittlement has been attributed to the inability of the liquid metal to penetrate the oxide and wet the solid substrate.

Failures produced by liquid-metal embrittlement have been reported to be both transgranular and intergranular. BCC and some HCP metals possess low-energy cleavage planes and, therefore, are prone to transgranular failure in the presence of this environment. In single-phase FCC solids, however, there is no low-energy crystal plane for cleavage, so that the fracture almost invariably follows the grain boundaries.

Object

Preliminary tests suggested that copper-contamination cracking (CCC) may be a form of liquid-metal embrittlement.[1] If this is indeed so, there are a number of tests which can be conducted to determine if the cracking process conforms to the criteria established by others for liquid-metal embrittlement.

Since Cu is the most popular material for the construction of weld tooling, it is particularly important to gain a thorough understanding of this form of cracking. In addition to the potential contribution to the field of liquid-metal embrittlement, the investigation of this problem therefore has great practical significance.

In order to establish the mechanism of CCC, the effect of the following variables was determined: atmosphere, amount of Cu, stress, grain size, temperature, strain rate, and crack velocity.

Procedure

This investigation involved the use of the Gleeble testing device (which synthesizes conditions experienced in the actual weld[10,11]) to determine the influence of different variables on the CCC in laboratory specimens. In particular, the experiments were undertaken to determine if the CCC in the weld heat-affected zone conformed to the following experimental observations normally associated with liquid-metal embrittlement (LME):

1. The minimum temperature for LME is the melting point of the embrittling metal.
2. An adherent oxide layer on the surface of the solid base metal prohibits LME unless the liquid metal can reach the surface of the base metal through cracks in the layer.
3. The length of LME cracks is proportional to the volume of liquid metal present on the base metal.
4. The liquid-metal atoms must be continually supplied to the advancing crack tip for a LME crack to propagate in materials which are not notch sensitive.
5. LME can only occur after a finite amount of plastic deformation of the base metal.
6. The yield stress and strain-hardening rate of the base metal are unaffected by LME prior to fracture.
7. The fracture stress of FCC materials, although normally not dependent on grain size, is grain-size dependent when the grain boundaries are wet by certain liquid metals.
8. The susceptibility to LME decreases with increasing temperature. A brittle-to-ductile transition is generally reported for LME of FCC materials at some temperatures above the melting point of the embrittling metal.
9. The susceptibility to LME in-

Table 1—Summary of the Alloys and Their Nominal Compositions Used in This Investigation, %

Material	C	Fe	Cr	Ni	Co	Other
AISI Type 304	0.067	Bal	18.3	8.65	—	1.68 Mn, 0.51 Si
AISI Type 316	0.15 max	Bal	16–18	12–14	—	2.0 Mn max, 1.5-2.5 Mo
AISI Type 321	0.08 max	Bal	17–19	8–11	—	Ti = 5C
AISI Type 347	0.12 max	Bal	18–19.5	10–14	—	2.0 Mn max, Cb + Ta = 10C, 1.5 max
AISI Type 410	0.05–.15	Bal	11.5–13.5	0.5 max	—	1.0 Mn max, 0.5 Mo max
AISI Type 430	0.12 max	Bal	14–18	—	—	
Inconel 718	0.08	18.30	18.93	Bal	0.11	3.02 Mo, 0.62 Al, 0.88 Ti, 5.16 Cb + Ta
L-605	0.10	—	20.0	10.0	Bal	15.0 W
Haynes 188	0.10	1.4	21.82	21.87	Bal	13.83 W
Autobody stock	0.055	Bal	0.01	0.05	—	0.33 Mn, 0.01 Mo

creases with increasing strain rate.

10. The LME crack velocity varies inversely with crack length and has been reported to approach velocities of 500 cm/second(s).

11. The LME fracture in FCC materials is always intergranular.

Materials

Table 1 lists the nominal composition of the alloys used to determine the mechanism of CCC.

Testing Procedure

The Gleeble was used to perform all the high-temperature mechanical testing throughout this investigation. Unless otherwise specified, all tests were performed in an atmosphere chamber filled with prepurified 99.998% argon to protect the specimen from oxidation. A quenching operation, programmed to spray quench the specimen at 75,000 F/s (41,700 C/s) from any point in the thermal cycle, was used in certain tests.

Copper Plating Procedure

A standard acid plating bath was used to plate the specimens with 100% current efficiency. The thickness of the plate was regulated by adjusting the time of plating for a given current density. Details of this Cu-plating technique are given in a previous report.[1]

Results and Discussion

Determination of the Minimum Temperature for Copper-Contamination Cracking

To establish the minimum temperature at which CCC occurs, a series of short-time, constant-load, stress-rupture tests were conducted for two Fe-base alloys (Types 304 and 316) and a Co-base alloy (Haynes Alloy 188). Both Types 304 and 316, which are FCC at all test temperatures, exhibit markedly decreased times-to-rupture at all temperatures above the melting point of Cu, whenever Cu is present.

Inspection of Fig. 1 reveals that the time-to-rupture for the Type 304 plated specimen tested at 2030 F (1110 C) was only 7.6 s compared to 1100 s for the unplated control specimen. This reduction in rupture life by a factor of 145 is conclusive evidence that Type 304 is susceptible to CCC. It is important to note, however, that for both Types 304 and 316, the presence of Cu had no significant effect on the stress-rupture life at temperatures below the melting temperature of Cu.

Similar results were obtained with Haynes 188, a FCC Co-base alloy. This alloy was also extremely sensitive to the presence of Cu at all temperatures above the melting temperature of Cu and insensitive below the melting point of Cu.

Figure 2 shows the appearance of a typical unplated control specimen and a specimen of a material susceptible to CCC after testing at 2060 F (1127 C). Note the marked reduction in area exhibited by the control specimen and the extensive transverse cracking in the Cu-plated specimen.

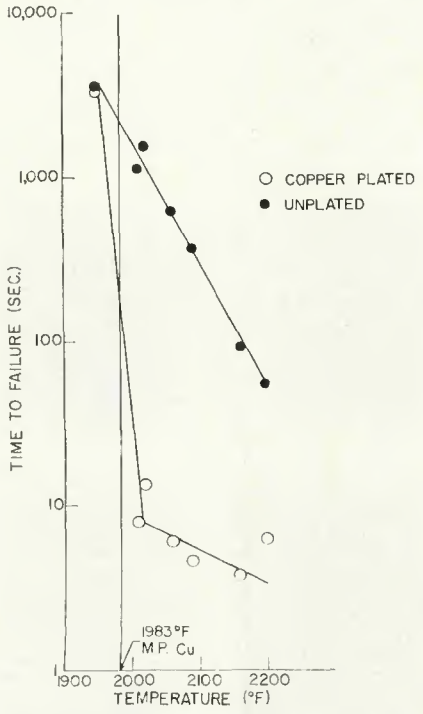

Fig. 1—Time-to-failure vs. temperature for constant-load stress-rupture testing of Type 304 stainless steel loaded at 3500 psi initial stress

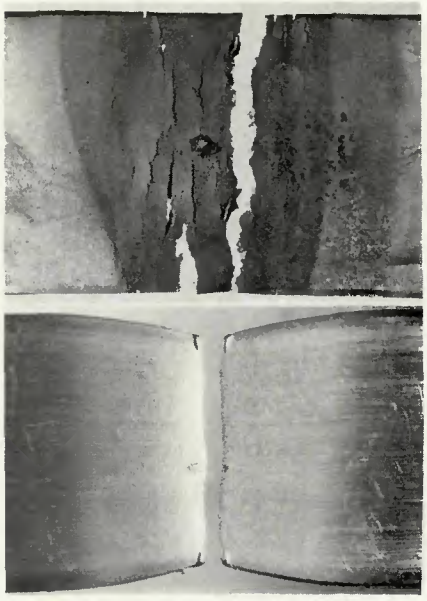

Fig. 2—As-fractured Type 304 stainless steel specimens tested at 2060 F with a constant elongation rate of 0.023 ips: A (top)—copper-plated specimen; B (bottom)—unplated control specimen. ×3 (reduced 50% on reproduction)

The Effects of Heating Time and Atmosphere

A series of experiments was performed to determine the effect of heating rate on the elevated-temperature hot-ductility of plated specimens of Type 304. Specimens with a 0.0714 mil (1.8 μm) thick Cu plate were heated in air to 2070 F (1132 C) in 0.5, 5 and 10 s and then subjected to a constant elongation rate of 0.5 ips (12.7 mm/s) until failure occurred.

The specimens heated to test temperature in 5 and 10 s showed no evidence of CCC, whereas the specimen heated to test temperature in 0.5 s showed considerable cracking and almost no ductility. Unfortunately, it was not clear whether the absence of CCC associated with the slower heating rates was a result of volatilization or oxidation of the Cu plate.

Therefore, a second series of tests was conducted in which unplated and plated specimens were tested both in air and in an Ar atmosphere following heating to 2070 F (1132 C) in 5 s. As shown in Figs. 3A and B, the unplated control specimens tested in air and in Ar both displayed lateral contraction of approximately 21% and a reduction in area at the fracture surface of nearly 100%. The control specimen tested in air had a visibly thicker oxide film but otherwise was identical in appearance to that tested in Ar.

However, the fracture behavior of the Cu-plated specimens was affected by the atmosphere. Note that the fracture appearance of the plated specimen tested in air, Fig. 3C, was nearly identical to that of the control specimen tested under similar conditions. By contrast, when tested in argon, the plated specimens showed strong evidence of CCC (Fig. 3D) with no measurable lateral contraction and a vanishingly small reduction in area. Scanning electron microscopy of the fracture surface of the plated specimen tested in argon showed that the fracture was completely intergranular. The results of this test indicate that the CCC does not occur after prolonged exposure to an oxidizing environment because the Cu is rapidly converted to oxides. Therefore, CCC can only occur with welding processes which provide adequate shielding protection of the weld heat-affected zone to prevent oxidation of the Cu prior to its being liquefied by the temperature cycles associated with the weld traverse.

The Effect of the Volume of Copper Available

During the liquid-metal embrittle-

ment process, liquid-metal atoms must be present at the crack tip for propagation to continue in materials which are not notch sensitive. Because liquid-metal atoms must be continually supplied to the crack tip, the volume of Cu on the surface of the specimen should affect the severity of embrittlement by controlling the maximum depth of the CCC.

Typical examples of the effect of the volume of Cu plated on the surfaces of Type 347 on the hot-ductility behavior at 2165 F (1185 C) are shown in Fig. 4. Note that as the thickness of Cu increases from 0.003 mils (0.076 μm) in Fig. 4A, to 0.0238 mils (0.6 μm) in Fig. 4B, to 0.1904 mils (4.84 μm) in Fig. 4C, a progressive reduction in lateral contraction occurs. Figure 4D is a photomacrograph of the failure surface of the specimen shown in Fig. 4C. The light rim around the darker central position of the cross-section delineates the maximum depth to which the Cu rapidly penetrated the grain boundaries during testing. Thus the effective load-carrying area of the specimen is reduced to that of the darker appearing central core during the initial stages of the test.

Both the number and depth of cracks increased as the Cu thickness was increased up to 0.048 mils (1.2 μm). For greater thicknesses, the depth of cracking also increased, but the number of cracks decreased. Figure 5 summarizes, in graphical form, the effect of the plating thickness on the maximum crack depth.

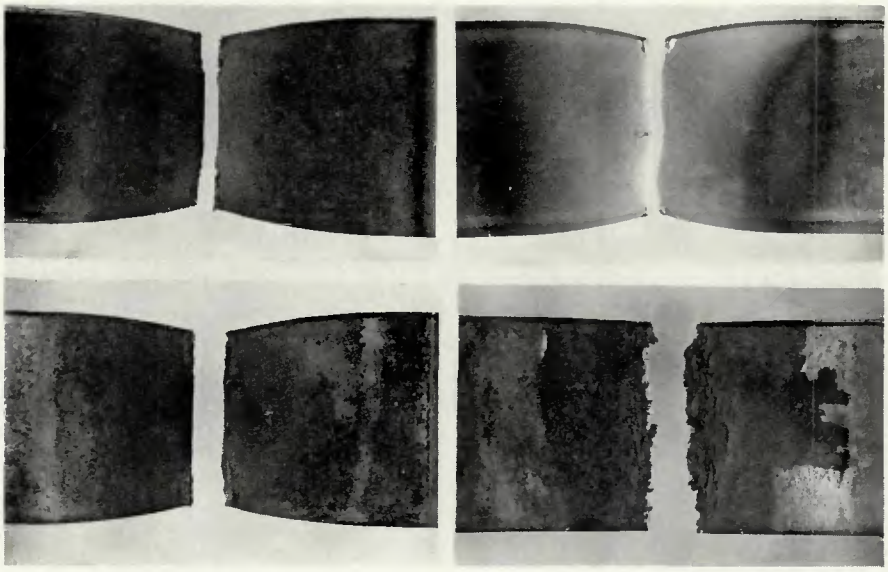

Fig. 3—As-fractured Type 304 stainless steel specimens tested in controlled atmospheres: A (top left)—unplated control specimen tested in air; B (top right)—unplated control specimen tested in argon; C (bottom left)—copper-plated specimen tested in air; D (bottom right)—copper-plated specimen tested in argon. ×2.25 (reduced 50% on reproduction)

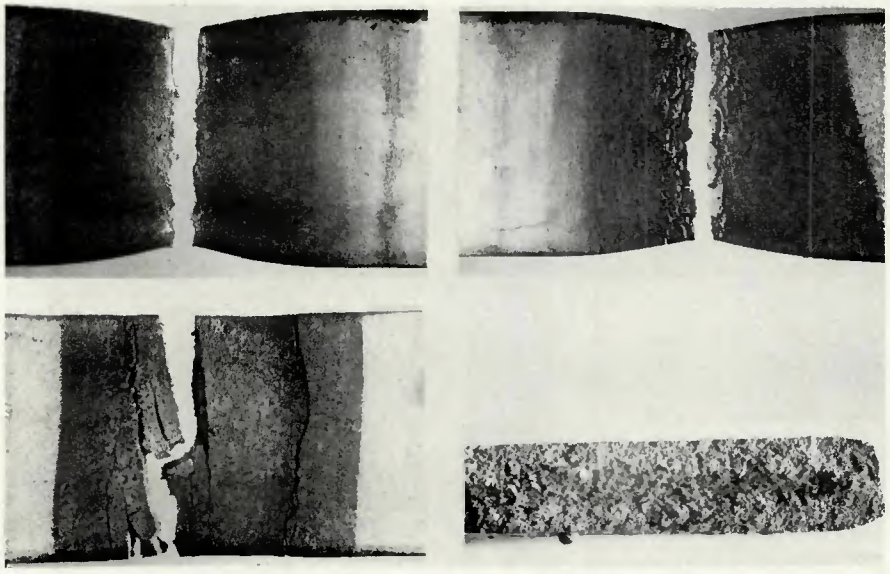

Fig. 4—As-fractured Type 347 stainless steel specimens tested at 2165 F with a constant elongation rate of 0.132 ips with differing thickness of the copper plate: A (top left)—0.003 mil thick copper; B (top right)—0.0238 mil thick copper; C (bottom left)—0.1904 mil thick copper; D (bottom right)—fracture surface of specimen tested with a 0.1904 mil thick copper plate. ×2.75 (reduced 50% on reproduction)

The Distribution of Copper

The fracture surfaces of several specimens which had been embrittled by CCC were examined with an energy-dispersion X-ray analysis (EDXA) system in a scanning electron microscope (SEM) to determine the Cu distribution on the fracture surface.

Figure 6 is an SEM photograph of the fracture surface of a plated Type 316 specimen which was tested in the Gleeble at 2165 F (1185 C). The features on the fracture surface of this specimen are typical of that observed with all Cu-plated specimens which experienced CCC. The intergranular brittle fracture extends from the surface (line A-A), into the base metal to a position identified by line B-B. The failure mode changes to a ductile-shear failure at this position, which locates the brittle-to-ductile transition in the failure mode. It should be noted that the depth to which the intergranular brittle fracture extends into the Type 316 base metal corresponds to the crack depth discussed in the previous section.

The fracture surface of the Cu-plated Type 347 specimen previously shown in Fig. 4D was subjected to EDXA at 18 locations within a 0.042 in. (1.07 mm) span. This span included a portion of the ductile fracture, the entire transition region, and some 0.030 in. (0.76 mm) of brittle fracture. The EDXA unit was programmed to print out the cumulative Cu K_α counts obtained at each location during the counting interval required to accumulate a standard count for Fe K_α. These data are summarized in Fig. 7, where the cumulative Cu K_α count is plotted as a function of location on the fracture surface.

The data indicate that Cu was present throughout the region of the fracture surface which had been embrittled by Cu and was in significantly less concentration on regions of the fracture surface which were not embrittled. This indicates that liquid Cu must be present at the crack tip for the CCC to propagate in the Type 304 steel which is not notch sensitive. Such a conclusion is in accord with other experimental results reported by investigators of liquid-metal embrittlement.

The Effect of Stress

Four alloys—Inconel 718, Types 430 and 304 stainless steels and L-

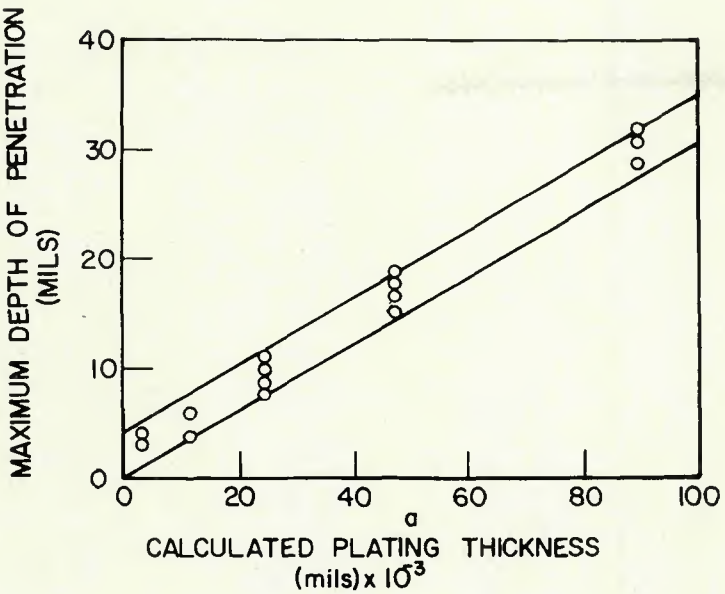

Fig. 5—Crack length vs. copper-plate thickness for Type 347 stainless steel specimens tested at 2165 F with a constant elongation rate of 0.132 ips

Fig. 6—Scanning electron photomicrograph of the fracture surface of a copper-plated Type 316 stainless steel specimen showing typical features observed on the fracture surfaces of alloys susceptible to copper-contamination cracking. ×125 (reduced 50% on reproduction)

605—were subjected to hot-ductility tests to determine the effect of stress on CCC. The results of these tests, expressed as engineering stress vs. elongation, of control and Cu-plated specimens are identical for both the Inconel 718 and the Type 430 stainless steel using an elongation rate of 0.132 ips (3.35 mm/s) at 2070 F (1132 C). Therefore, the presence of liquid Cu on the surface of these alloys does not significantly alter their mechanical behavior at 2070 F (1132 C). However, the presence of Cu does affect the elevated-temperature mechanical behavior of both Type 304 and L-605.

Note that when tested at 2040 F (1116 C) the behavior of the control and Cu-plated Type 304 specimens in Fig. 8 was identical throughout the elastic region, past the proportional limit, up to a critical stress level in the plastic region. Above this critical stress, the stress-elongation curve for the Cu-plated specimen suddenly deviates from that of the control specimen. The Co-base L-605 exhibited a similar behavior.

Returning to Fig. 8, note that the total elongation of the Type 304 at fracture was 242 mils (6.15 mm) for the unplated control specimen, 128 mils (3.25 mm) for the specimen with a 0.0714 mil (1.8 μm) thick plate (curve a), and 56 mils (1.4 mm) for the specimen with a 0.119 mil (3 μm) thick Cu plate (curve b). In addition, the area under the stress-elongation curves indicates that the presence of Cu in increasing amounts severely limits the total energy required to fracture the Type 304. This phenomenon can be explained as follows:

1. The depth of the CCC was greater in the specimen with the thicker Cu plate.

2. The total extension of the CCC occurs during an infinitesimally small initial portion of the plastic deformation at the critical stress.

3. For the plated specimens, the load-elongation trace beyond the critical stress represents the deformation of underlying, unembrittled base metal.

4. The greater crack depths associated with thicker Cu plating causes a greater reduction in the effective cross-sectional area of the remaining load-carrying portion of the specimen and, thus, localizes the plastic deformation to regions beneath the CCC.

5. In general, the greater the depth of CCC, the more the deformation will be localized, and the less total elongation will be experienced prior to fracture.

The Effect of Grain Size

In liquid-metal embrittlement, the fracture stress of FCC metals whose fracture stress is normally independent of grain size suddenly becomes size dependent when wet with certain liquid metals. To determine if this is the case with CCC, both coarse- and fine-grained specimens of the same heat of Type 304 were subjected to hot-ductility tests at 2165 F (1185 C) with an elongation rate of 0.125 ips (3.18 mm/s). The fine-grained specimens had an ASTM Grain Size #7.5 ($d = 1.05 \times 10^{-3}$ in., 0.027 mm) and the coarse-grained specimens had an ASTM Grain Size of approximately #2.0 ($d = 7.07 \times 10^{-3}$ in., 0.18 mm).

The ultimate tensile strength of the unplated control specimens decreased from 5,850 psi (4.11 kg/mm^2) for the fine grain size to 5,600 psi (3.94 kg/mm^2) for the coarse grain size, a decrease of only 4.3%. However, the ultimate tensile strength of the Cu-plated specimens decreased from 3,150 psi (2.21 kg/mm^2) for the fine-grained specimen to 2,100 psi (1.48 kg/mm^2) for the coarse-grained specimens, a decrease of 33.4% for an increase of approximately seven fold in grain diameter.

An additional specimen was tested whose grain size was coarsened by heat treatment in air rather than the argon environment used with the grain-growth heat treatments for all other grain-coarsened specimens. The adherent oxide formed on the surface of the specimen treated in air was not completely removed in this case. Therefore, the specimen was tested with the Cu layer plated over the adherent oxide layer. The tensile strength of this specimen (4,100 psi, 2.88 kg/mm^2) was intermediate between that of the unplated control sample (5,600 psi, 3.94 kg/mm^2) and the Cu-plated specimen (2,100 psi, 1.48 kg/mm^2). Apparently, a finite amount of strain is required for rupturing the intervening oxide film to allow the molten Cu to contact the underlying metal surface and cause embrittlement.

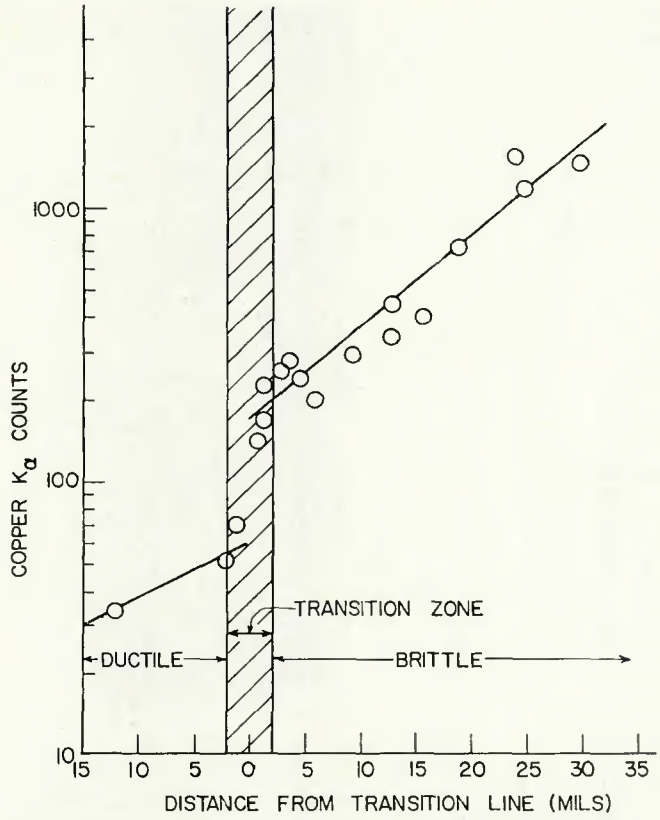

Fig. 7—EDXA Cu K_α counts vs. position on fracture surface of Type 347 stainless steel after embrittlement by copper-contamination cracking

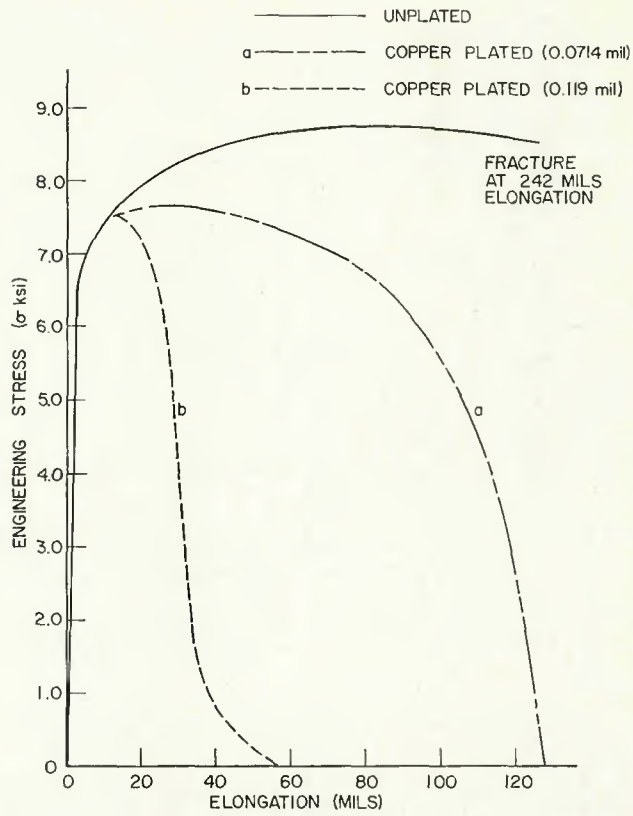

Fig. 8—Engineering stress vs. elongation for copper-plated and unplated control specimens of Type 304 stainless steel tested at 2040 F with a constant elongation rate of 0.132 ips

The Effect of Temperature

The susceptibility to liquid-metal embrittlement generally increases with decreasing temperature down to the melting point of the embrittling metal. To investigate the influence of temperature on CCC, both unplated control and plated Type 304 specimens were subjected to hot-ductility testing at various test temperatures.

The results are summarized by the photomacrographs of the as-fractured specimens presented in Fig. 9. The photomacrographs show a change in surface luster from a dark-colored region at the center near the thermocouple location to a bright region on either side of this dark band. Temperature measurements indicate that the boundary between the regions of dark and bright surface corresponds to the location at which the temperature just reached the melting point of Cu.

Note that in the specimen tested at 2030 F (1110 C) (Fig. 9A), the CCC is concentrated at the thermocouple location and the specimen shows a complete loss of ductility. However, at 2165 F (1185 C) (Fig. 9B) the cracking was no longer located near the thermocouple, but near the edge of the dark region where the temperature was only slightly above the melting point of Cu. The region of the specimen near the thermocouple location was devoid of any CCC. In the specimen tested at 2270 F (1243 C) (Fig. 9C), the CCC was again located near the edge of the dark region and the center of the specimen began to show some ductility.

At higher test temperatures—2380 F (1304 C), 2480 F (1360 C), and 2530 F (1388 C)—the cracking was always located near the edge of the dark region where the temperature was only slightly above the melting point of Cu, as shown in Fig. 9D for 2480 F (1360 C). The increase in the width of the region experiencing temperatures above the melting point of Cu makes the necking caused by localized yielding of the hotter, weaker material near the center more evident.

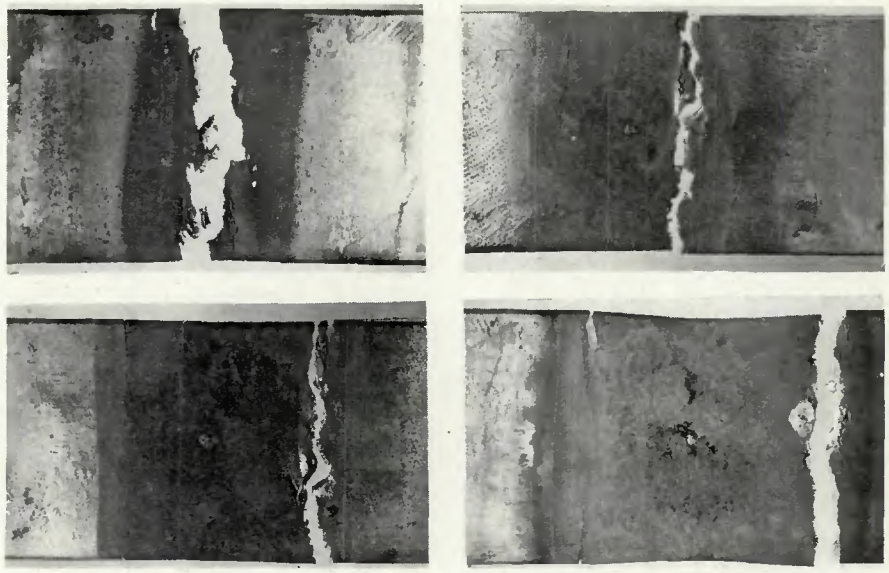

Fig. 9—As-fractured copper-plated Type 304 stainless steel specimens tested with a constant elongation rate of 0.023 ips at differing test temperatures: A (top left)—2030 F; B (top right)—2165 F; C (bottom left)—2270 F; D (bottom right)—2480 F. ×2.5 (reduced 50% on reproduction)

To determine if the lack of embrittlement in the regions near the thermocouple was caused by either a volatization or a volume-diffusion mechanism which eliminated the Cu layer, a second experiment was performed. In this case, a plated Type 304 specimen was heated to 2480 F (1360 C) in 10 s, held at temperature for 10 s, cooled to 2030 F (1110 C), and pulled to fracture at a constant elongation rate of 0.023 ips (0.58 mm/s) at 2030 F (1110 C).

The 10 s holding time at temperature simulated the actual time at 2480 F (1360 C) during the original hot-ductility tests. The fracture was again located in the central portion of the specimen at the thermocouple location, and the specimen showed no ductility. This proves conclusively that neither volatization nor volume diffusion of Cu could have been a significant factor in the original hot-ductility testing because these processes would not be reversible during cooling from 2480 F (1360 C) to the final test temperature of 2030 F (1110 C).

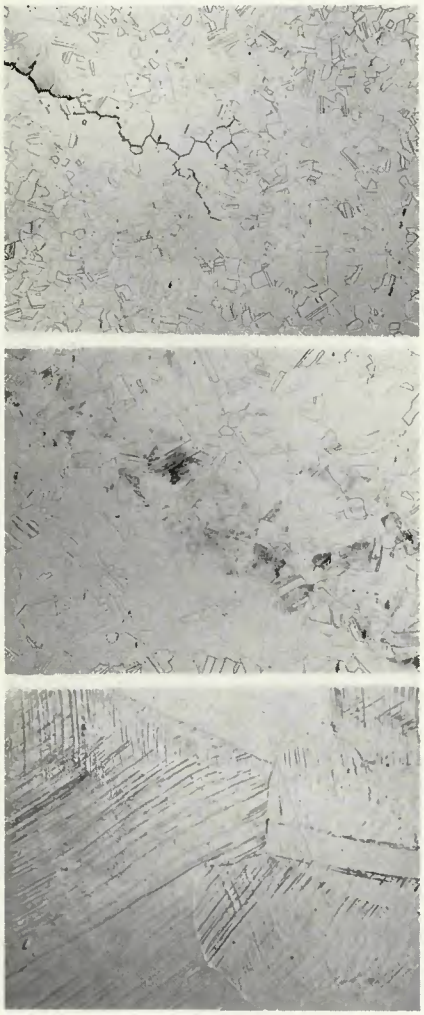

Fig. 10—Microstructure of a Type 304 stainless steel specimen embrittled by copper during a hot-ductility Gleeble test at 2380 F: A (top)—location of the copper contamination cracking, ×100; B (middle)—center of the specimen at the thermocouple location, ×100; C (bottom)—center of the specimen at the thermocouple location, ×750 (reduced 50% on reproduction)

Metallographic Examination

The specimen tested at 2380 F (1304 C), previously shown in Fig. 9D, was examined metallographically. Photomicrographs at ×100 were taken at the location where the CCC occurred (Fig. 10A) and at the center of the specimen where the thermocouple was located (Fig. 10B). The grain size at the thermocouple location is considerably larger than that at the CCC location, as a result of exposure to temperatures at which rapid grain growth occurs.

The fact that the cracking occurs preferentially where the temperature is only slightly above the melting point of Cu indicates that the higher temperature portions of the specimen must be less sensitive to the embrittlement by liquid Cu. The photomicrographs in Figs. 10B and 10C (taken at ×100 and ×750, respectively) show the microstructure in the vicinity of the thermocouple in the specimen tested at 2380 F (1304 C). The evidence of planar slip on multiple slip systems in the band running diagonally from the upper left to lower right corner in Fig. 10B can be clearly resolved in Fig. 10C. Such planar slip is often observed following plastic deformation of face-centered cubic metals with low stacking-fault energies.

It appears thus, that the yield strength of the hotter material near the center of the specimen is initially below the critical stress required to cause CCC in the lower temperature regions near the edge of the dark band. However, as the hotter central region which is insensitive to CCC, deforms plastically, strain hardening results until the nominal stress in the specimen reaches the critical level and CCC then occurs in the lower temperature region near the outer edge of the dark band.

To eliminate the effect of the temperature gradient on the location of CCC in hot-ductility tests, Type 304 specimens were prepared with a band of Cu plate, only ⅛ in. (3.2 mm) wide centered about the thermocouple location. Because the temperature distribution was constant within ± 15 F (± 8 C) over a region of approximately

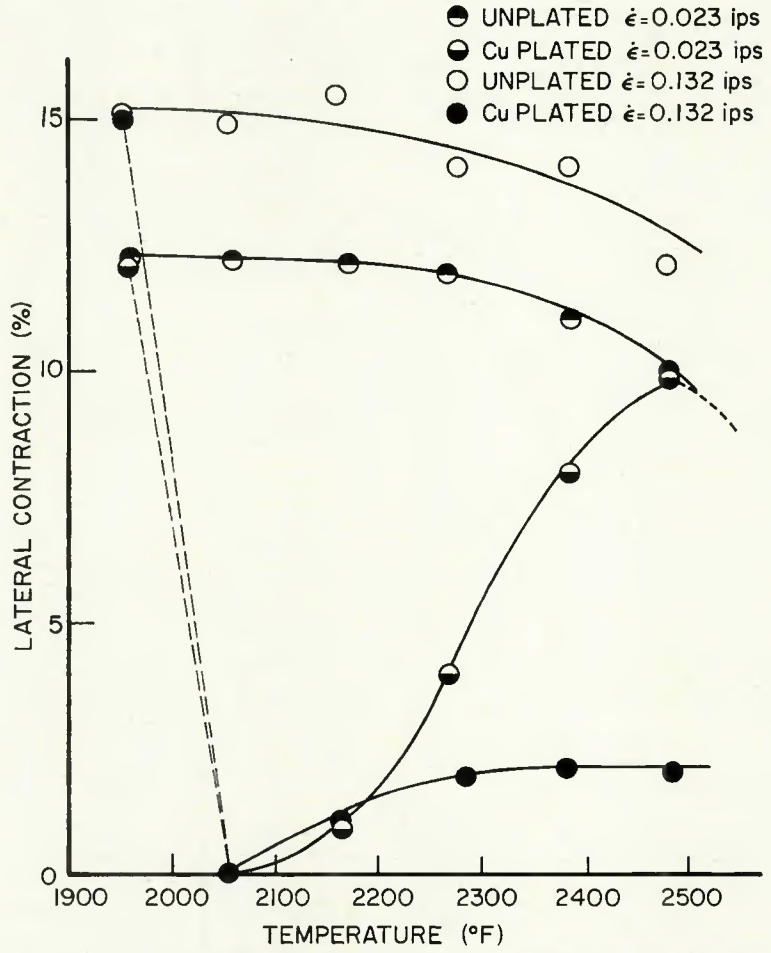

Fig. 11—Lateral contraction vs. temperature for copper-plated and unplated control specimens of Type 304 stainless steel tested with a constant elongation rate of 0.023 ips and 0.132 ips

Table 2—Summary of Capillary-Transport Calculations for Liquid Copper in Iron

Crack length		Capillary velocity		Transport
cm	in.	cm/s	in./s	time, s
0.001	0.000394	457.	180.	1.09×10^{-6}
0.005	0.00197	91.5	36.0	2.73×10^{-5}
0.01	0.00394	45.7	18.0	1.09×10^{-4}
0.02	0.00787	22.9	9.0	4.37×10^{-4}
0.03	0.0118	15.2	6.0	9.84×10^{-4}
0.04	0.0157	11.44	4.5	1.75×10^{-4}
0.05	0.0197	9.15	3.6	2.73×10^{-3}
0.10	0.0394	4.57	1.8	1.09×10^{-2}
0.50	0.197	0.915	0.36	2.73×10^{-1}

¼ in. (6.4 mm) wide, the effect of temperature on CCC could be more accurately evaluated.

The results of this investigation are shown in Fig. 11 for two strain rates—0.023 and 0.132 ips (0.58 and 3.35 mm/s). Note that the ductility of the Cu-plated specimens falls precipitously to zero between 1960 and 2060 F (1071 and 1127 C) and then, for the slower strain rate, rises sigmoidally with increase in testing temperature until 2480 F (1360 C). At this temperature, the ductilities of the unplated and the plated specimens are the same.

In order to determine if the sigmoidal return of ductility evident in Fig. 11 could be related to a phase transformation of the FCC austenite to BCC delta ferrite, an additional series of tests were conducted. A series of specimens were heated to test temperatures in the range from 2270 to 2530 F (1243 to 1388 C) in 10 s, held for times of 0, 5, 30, and 60 s, and then water-spray quenched at approximately 75,000 F/s (41,700 C/s).

Metallographic examination of the potentiostatically etched specimens revealed no delta ferrite below 2530 F (1388 C), at which temperature a network of ferrite was produced at the austenite boundaries.

In addition, a differential thermal analysis of the Type 304 steel established the delta ferrite transformation temperature as 2512 F (1378 C). This is offered as additional proof that delta ferrite could not have been present in the specimens or have been a factor in the low-strain rate brittle-to-ductile transition which occurred in the Type 304 between 2060 and 2480 F (1127 and 1360 C).

The Effect of Strain Rate

Because the shear stress increases with higher strain rates, it is conceivable that increased strain rates could affect σ/τ (the embrittlement susceptibility ratio) such that a material, which is normally insensitive to liquid-metal embrittlement, could be rendered sensitive. To investigate this possibility, the hot-ductility tests described in the preceding section were utilized to determine the influence of strain rate on the brittle-to-ductile transition. The results of these tests are shown in Fig. 11.

Note that the Type 304 was rendered brittle throughout the temperature range of 2000 to 2480 F (1093 to 1360 C) at the higher elongation rate of 0.132 ips (3.35 mm/s). Instead of the complete recovery of ductility noted at 2480 F (1360 C) with the slower strain rate, 0.023 ips (0.58 mm/s), only partial recovery was observed at the faster elongation rate. This indicates that the susceptibility to the CCC in the Type 304 in the temperature range investigated increases with an increase in strain rate. Because liquid Cu atoms must be continually supplied to the crack tip for CCC propagation, the rate at which liquid Cu can be transported to the crack tip may be the rate-controlling factor in CCC.

Rearranging equation (1) for the capillary-transport velocity:

$$LdL = \frac{T\ r\ \cos\theta}{3\pi\mu}\ dt \qquad (2)$$

Assuming all integration constants to be zero, the expression then becomes:

$$L^2 = \frac{2T\ r\ \cos\theta}{3\pi\mu}\ t \qquad (3)$$

Assuming the surface tension of liquid Cu (T) to be 1300 dynes/cm, the effective width of the crack (r) to 1.20×10^{-4} cm, the contact angle (θ) to be 20°, and the coefficient of viscosity (μ) to be 0.034 poise, equation 3 reduces to:

$$L^2 = 0.915t \qquad (4)$$

The results of calculations using equations (1) and (4) are listed in Table 2. Note that this transport mechanism is capable of sustaining extremely fast velocities for short crack distances.

To compare the CCC velocities with the calculated capillary-transport velocities, a series of plated Type 304 specimens were subjected to hot-ductility tests at 2160 F (1182 C) with constant elongation rates up to 12.88 ips (327 mm/s). The crack depths increased slightly as the temperature decreased from the thermocouple position, to the position where the temperature was only slightly above the melting point of Cu and the susceptibility to CCC the greatest.

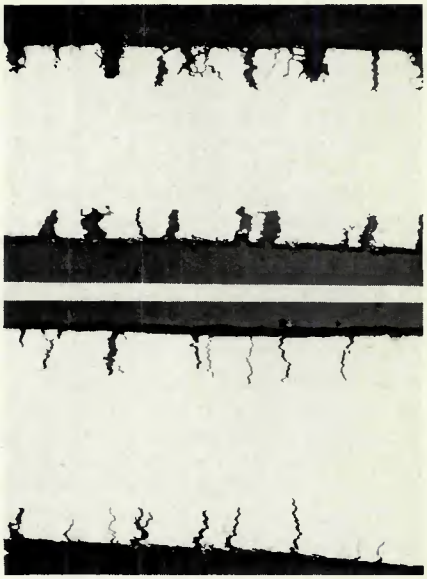

Fig. 12—Longitudinal sections of copper-plated Type 304 stainless steel specimens tested at 2160 F with a constant elongation rate of 12.88 ips: A (top)—central portion, temperature 2160 F; B (bottom)—position removed from thermocouple, temperature approx. 2000 F. ×50 (reduced 50% on reproduction)

Photomicrographs at ×50 of a longitudinal section of the fractured specimen near the thermocouple (2160 F, 1182 C) and near the region where the temperature was slightly above the melting point of Cu (1982 F, 1083 C) are shown in Fig. 12A and B, respectively. Because adjacent crack faces tend to match across the cracks in both Fig. 12A and B, the cracks must have extended to their final length prior to being torn-open or "blunted" and prior to any significant amount of plastic deformation of the underlying base metal.

During the 12.88 ips (327 mm/s) hot-ductility test, the total time for plastic deformation in the specimen was only 0.0256 s. According to the photomicrographs in Fig. 12, the crack lengths varied from 8.76 to 11.9 mils (0.22 to 0.3 mm). Using capillary-transport calculations (examples of which are shown in Table 2), the total time necessary to transport liquid Cu to those depths in the base metal would have varied from 5.41×10^{-4} to 9.98×10^{-4} s. Even assuming the longest propagation time, this represents less than 4% of the total time the specimen was experiencing plastic

deformation. Therefore, capillarity could well have produced the CCC observed in the specimen tested at 12.88 ips (327 mm/s).

Fracture Morphology

Alloys that were embrittled by liquid Cu were examined by both optical and scanning electron microscopy (SEM) to determine the fracture mode and to deduce the failure mechanism of the CCC. As an example, Figs. 13A and B constitute a photomicrograph of a longitudinal section and a SEM photograph, respectively, of the fracture surface of a specimen of Haynes 188. Note that both methods of examining the fracture morphology indicate that the fracture was completely intergranular.

The SEM photograph in Fig. 13B indicates that the CCC occurs predominantly by intergranular cleavage in the Haynes 188. However, a few isolated grain faces were not cleaved, but rather failed by intergranular shear. Because the liquid Cu must be transported from the surface of the specimen to the crack tip, it seems reasonable that some isolated grain boundaries may not be wetted by copper in the short time of the test.

The second phase visible in Fig. 13A is an M_6C carbide precipitate[12] which is stable to above 2400 F (1316 C). These carbides are also apparent along the grain faces in the scanning electron photomicrograph—Fig. 13B. Holes in the fracture surface are also noted which indicate the position of carbides which have been pulled out and remained on the matching fracture surface of the specimen.

In addition, the examination of fracture morphologies associated with CCC in Types 304, 316, 321, and 347 stainless steels, HY-80 steel, AISI 4130 and AISI 4340 steels, and auto-body stock all revealed a predominantly intergranular fracture. Therefore, the fractures observed in a wide variety of Fe- and Co-base alloys which resulted from CCC were all intergranular. It is interesting to note that all these alloys that were sensitive to CCC had a FCC structure at the melting point of Cu.

Summary

The observations noted in this investigation are all consistent with the phenomenological behavior identified as liquid-metal embrittlement, as outlined previously under **Procedure**. In particular, the brittle-to-ductile transition noted in the Cu-contaminated Type 304 stainless specimens (Fig. 11) is considered the critical experimental result which proves that the mechanism responsible for copper-contamination cracking is liquid-metal embrittlement by liquid Cu.

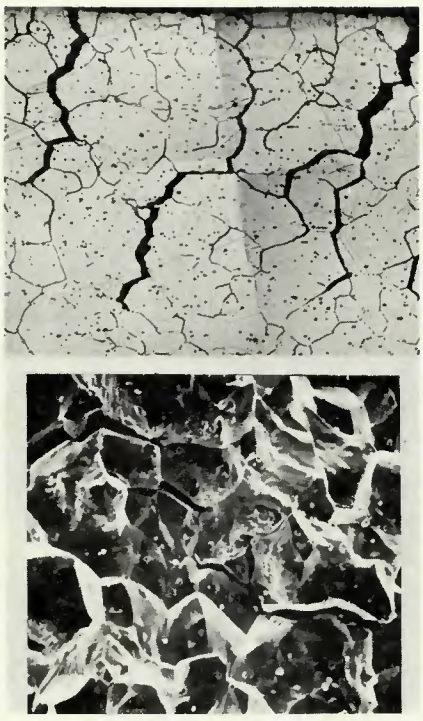

Fig. 13—As-fractured copper-plated Haynes 188: A (top)—optical photomicrograph of longitudinal section, ×200; B (bottom)—scanning electron photomicrograph of fracture surface, ×500 (reduced 50% on reproduction)

Liquid-metal embrittlement has only been observed in the FCC metals.

Conclusions

The cracking of the weld heat-affected zone remote from the fusion boundary was analyzed and found to be a result of liquid-metal embrittlement by liquid Cu on the surface of the test specimens. This form of hot cracking was observed with a layer of Cu only 0.003 mil (0.076 μm) thick on the surface of alloys susceptible to this form of liquid-metal embrittlement. Such minute quantities of metal could easily have been introduced as a contaminant through abrasion with Cu or Cu-alloy weld tooling.

The following conclusions have been drawn concerning the copper-contamination cracking of the weld heat-affected zone in Co- and Fe-base alloys which have a FCC structure at the melting point of the Cu phase:

1. The hot cracking is restricted to portions of the weld heat-affected zone where the temperatures are above the melting point of the embrittling Cu-contamination layer.

2. Hot cracking can occur if the welding process provides adequate shielding protection of the weld heat-affected zone to prevent oxidation of the Cu on the surface of the weldment.

3. The susceptibility to the Cu-induced hot cracking decreases with increased temperature above some transition temperature in the weld heat-affected zone.

4. The crack morphologies encountered in the weld heat-affected zone of FCC metals are intergranular and are oriented perpendicular to the principal-stress direction.

5. The hot-cracks propagate at high velocities once a critical amount of plastic strain is introduced in the weld heat-affected zone.

6. In materials which are not notch-sensitive, the liquid Cu must be present at the crack tip for the continued propagation of copper-contamination cracks.

References

1. Savage, W. F., Nippes, E. F., and Mushala, M. C., "Copper-Contamination Cracking in the Weld Heat-Affected Zone," *Welding Journal,* 57 (5), May 1978, Research Suppl., pp. 145-s to 152-s.

2. Stoloff, N. S., "Liquid Metal Embrittlement," *Surfaces & Interfaces, Vol. II,* Syracuse University Press, Syracuse, N. Y. (1968).

3. Westwood, A. R. C., Preece, C. M., and Kamdar, M. H., "Adsorption-Induced Brittle Fracture in Liquid-Metal Environment," *Fracture, Vol. III,* Academic Press, Inc., New York, N. Y., (1971) p. 589.

4. Kelly, A., Tyson, W. R., and Cottrell, A. H., "Ductile and Brittle Crystals," *Phil. Mag., 15,* (1967), pp. 567-586.

5. Stoloff, N. S., and Johnston, T. L., "Crack Propagation in a Liquid Metal Environment," *Acta Met., 11,* (1963), pp. 251-256.

6. Rostoker, W., McCaughey, J. M., and Markus, H., *Liquid Metal Embrittlement,* Reinhold Publishing Corp., New York, N. Y., (1960).

7. Perrone, N., and Liebowitz, H., "Effect of Capillary Action on Fracture Due to Liquid Metal Embrittlement," *Proceedings of the First International Conference on Fracture,* Sendai, Japan, (1965), p. 2065.

8. Semlak, K. A., and Rhines, F. N., "The Rate of Infiltration of Metals," *Trans. AIME, 209,* (1958), pp. 325-331.

9. Preece, C. M., and Westwood, A. R. C., "Temperature-Sensitive Embrittlement of FCC Metals by Liquid Metal Solutions," *Trans. ASM, 62,* (1969), pp. 418-425.

10. Nippes, E. F., and Savage, W. F., "Development of Specimen Simulating Weld Heat-Affected Zones," *Welding Journal,* 28 (11), Nov. 1949, Research Suppl., pp. 534-s to 546-s.

11. Savage, W. F., "Apparatus for Studying the Effects of Rapid Thermal Cycles and High Strain Rates on the Elevated Temperature Behavior of Materials," *Journal of Applied Polymer Science,* 6, (1962), pp. 303-31S.

12. Herchenroeder, R. B., Matthews, S. J., and Tackett, J. W., "A Versatile High-Temperature Alloy," *Metals Progress, 102,* (1972), pp. 60-64.